

Photocatalytic degradation of phenylephrine hydrochloride in aqueous solutions by synthesized SnO₂-doped ZnO nanophotocatalyst

Masoud Giahi*, Akram Hoseinpour Dargahi

Department of Chemistry, Faculty of Science, Lahijan Branch, Islamic Azad University, Lahijan, Iran.

Received 17 September 2015; received in revised form 22 December 2015; accepted 29 February 2016

ABSTRACT

ZnO and SnO₂-doped ZnO nanoparticles were prepared by a sol-gel method for the first time. X-ray diffraction (XRD) and scanning electron microscopy (SEM) were used to characterize the ZnO and SnO₂-doped ZnO samples. Advanced oxidation processes (AOPs) have proved very effective in treatment of the various hazardous organic pollutants such as surfactants and pharmaceuticals in water. The photocatalytic degradation of drug phenylephrine hydrochloride (PHE) was studied as model organic pollutant. Under UV exposure the process was investigated with ZnO and SnO₂-doped ZnO. The degradation was studied under different conditions including irradiation time, pH, catalyst concentration, phenylephrine hydrochloride concentration and potassium peroxydisulfate as an oxidant. The experimental results indicated that maximum degradation (99.4±1.0%) of drug occurred with SnO₂-doped ZnO catalyst. The results demonstrated that photodegradation efficiency of SnO₂-doped ZnO was significantly higher than that of undoped ZnO.

Keywords: SnO₂-doped ZnO, Phenylephrine hydrochloride, Potassium peroxydisulfate, Photocatalytic degradation.

1. Introduction

Polluted water imposes a serious threat to the environment. Besides, water pollutants such as pesticides, dyes and surfactants and pharmaceuticals are among emerging class of aquatic contaminants. Both human and veterinary pharmaceuticals have been increasingly detected in sewage water, natural water, surface water and ground water [1–5]. Recently, considerable attention has been focused on the use of semiconductor as a mean to oxidize toxic organic chemicals [6–11]. Photocatalysis is a promising technique for the degradation of inorganic and organic pollutants in air and water [12]. Especially, Semiconductor oxides such as ZnO and TiO₂ have been recognized to be preferable materials for photocatalytic processes, due to their high photosensitivity, non-toxic nature, low cost and chemical stability [13–15]. However, ZnO, and TiO₂ can only absorb a small portion of solar spectrum in the UV region, because of their wide band gaps [16]. On the other hand, ZnO is well known to semiconduct under solar irradiation, and its photocatalytic

mechanism has proved to be similar to that of TiO₂, although it shows less vigorous oxidation states [17]. ZnO has sometimes been reported to be more efficient than TiO₂. The biggest advantage of ZnO is that it absorbs over a larger fraction of the solar spectrum than TiO₂ [18]. In such semiconductors, photogenerated carriers (electrons and holes) could tunnel to a reaction medium and participate in chemical reactions. The high degree of recombination of these carriers greatly decreases their photocatalytic efficiency. Clearly, a wider separation of the electron and the holes increases the efficiency of photocatalyst. Fortunately, utilizing coupled oxide semiconductors could increase the charge separation and extend the energy range of photooxidation. In the past several years, coupled semiconductors formed by ZnO and other metal oxides or sulfides such as TiO₂, SnO₂, Fe₂O₃, WO₃, CdS, ZnS and so on have been reported [19–23]. Various semiconductor based heterostructure photocatalysts have been designed and investigated such as TiO₂-ZnO [24], TiO₂-WO₃ [25], and ZnO-WO₃ [26]. Among the binary metal oxides, tetragonal tin dioxide, SnO₂, is a well-known large band gap multifunctional material that found wide spread applications in the fields of Li-batteries [27], field emission [28], gas sensing [29], and photovoltaic

*Corresponding author email: m.giahi@liau.ac.ir
Tel.: +98 13 4222 2605

conversion [30]. Because of its more positive CB edge, SnO₂ is a better electron acceptor than TiO₂ and ZnO, which makes it a good candidate for the above-mentioned heterostructures. As a consequence, associating SnO₂ with ZnO has been the subject of several reports for achieving an efficient charge separation and improving the photocatalytic properties of both oxides [31-32]. The estimated band gap energies of the resulting samples were therefore about 3.7, 3.23, and 3.2 eV for SnO₂, SnO₂-ZnO, and ZnO, respectively. The values for ZnO and SnO₂ were in good agreement with those reported by others [33].

In this paper, we prepared the ZnO and SnO₂-doped ZnO photocatalysts by "sol-gel method". The photocatalytic degradation of phenylephrine hydrochloride (PHE) in the presence of SnO₂-doped ZnO nanopowder with UV light as the illuminate was then examined. The results showed that coupling of different semiconductor oxides could reduce its band gap, extend its absorption range to a visible light region, promote electron-hole pair separation under irradiation, consequently, achieve a higher photocatalytic activity [34].

2. Experimental

2.1. Materials

Phenylephrine hydrochloride powder (PHE: C₉H₁₃NO₂.HCl, Molar mass: 203.67g/mol) was obtained from Behdasht Kar Pharmacy. Zinc nitrate hexahydrate (Zn(NO₃)₂.6H₂O), Tin (II) chloride dihydrate (SnCl₂.2H₂O), ethylene glycol, citric acid, K₂S₂O₈ were from Merck. All reagents were used without further treatment.

2.2. Preparation of ZnO

In a typical procedure, 25 mL ethylene glycol was mixed with 6g Zinc nitrate, 25mL H₂O and 6.4 g citric acid under vigorous stirring for 4h. The prepared solution was kept at dark for 24h. Finally, the obtained gel was dried and calcined at 500°C for 3h.

2.3. Preparation of SnO₂ 10% mol doped ZnO

25 mL of ethylene glycol was mixed with 5.35g Zinc nitrate, 25ml distilled water and 6.3 g citric acid under vigorous stirring for 1h. After 15 min 0.45 g SnCl₂.2H₂O was added to suspension under vigorous stirring at 60 °C for 180 min. The prepared solution was kept at dark for one day. Finally, the obtained gel was dried and calcined at 500°C for 3 h.

The powder X-ray diffraction (XRD) patterns of the samples were recorded by a BRUKER D8 ADVANCE X-ray diffractometer using Cu-K α radiation, morphologies and element content were investigated by a JSM-6700F scanning electron microscopy (SEM).

2.4. Evaluation of photocatalytic activity

Photocatalytic experiments were carried out in the UV reactor equipped with cooling feature, magnetic stirrer and UV lamp. 36-W mercury lamp was used as the UV light source. The contact time, PHE solution with an initial concentration, initial pH, catalyst amount and K₂S₂O₈ concentration were selected as experimental parameters. The temperature was kept constant within (25 \pm 2) °C. In separate experiments, the suspension was magnetically stirred in the dark to reach a complete adsorption desorption equilibrium of PHE on the catalyst surface. The pH of the solution was adjusted by using a pH meter equipped with a combined electrode. The mixture was irradiated with the UV lamp. The aqueous suspension was magnetically stirred (at 64 rpm) throughout the experiment. Lastly, 5mL of the solution was centrifuged for 15 min at 4000 rpm and then the concentration of PHE in the supernatant was determined with a 1.0 cm light path quartz cells using spectrophotometer (Model Jenway 6405). Absorbance of the supernatant solution was measured and returned to the reactor. The amount of degradation was calculated from the concentrations in the solution before and after the experiments. The rate of degradation was considered in terms of change in absorption spectra at λ_{max} = 273 nm. The photocatalytic degradation efficiency was calculated from the following relationship: $X = (C_0 - C) / C_0$. Where, C₀ is the initial concentration of the pollutant, C the concentration of the pollutant and time t [35-37].

3. Results and Discussion

3.1. Characterization of photocatalysts

The XRD patterns of the as prepared pure ZnO and 10% SnO₂ doped ZnO are shown in Fig. 1. It can be seen from Fig. 1 that dominant structure in these samples is wurtzite ZnO (JCPDS CardNo.36-1451).

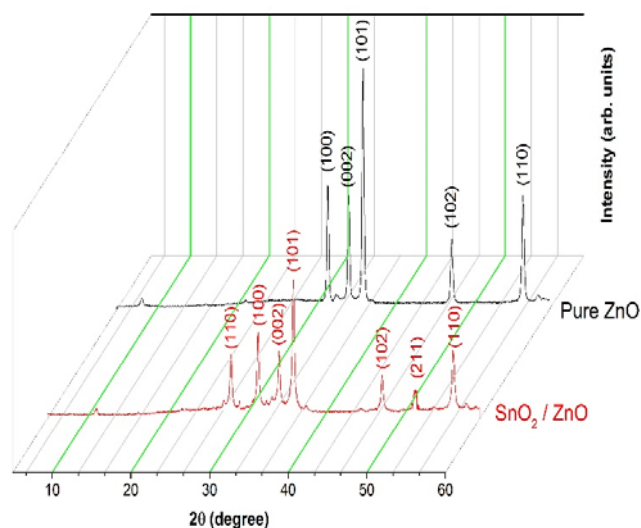


Fig. 1. XRD patterns of ZnO and 10%SnO₂/ZnO.

The distinguished peaks of the hexagonal Wurtzite ZnO structure with the angles of $2\theta = 31.8$ (direction of (100)), $2\theta = 34.5$ (preferable direction of (002)), and $2\theta = 36.3$ (direction of (101)) can be observed in this figure. Fig. 1b. shows that one probable reason is that the formula of nanoparticle (Zn_2SnO_4), which showed Sn doped in ZnO. It is worth noting that tin oxide related peaks were observed in the XRD spectra, $2\theta = 27.3$ (direction of (110)) and $2\theta = 51.7$ (direction of (211)). In addition, the diffraction peaks of ZnO and SnO_2 become sharper, indicating the increase of crystal size and improvement of crystallinity. By using the Debye-Scherrer equation, the crystallite sizes of ZnO and 10% SnO_2/ZnO were calculated to be 61.1 and 70.1 nm. The increase in the particle size of 10% SnO_2/ZnO is mainly attributed to the formation of Sn-O-Zn on the surface of the doped samples.

Fig. 2 shows the SEM images of the pure ZnO and 10% SnO_2 doped ZnO nanopowders prepared by sol-gel method. It was observed that in the case of 10% SnO_2 the grain size was bigger than the undoped ZnO. The SEM investigations of all samples revealed that the crystallites are of nanometer size. The SEM image showed that the average grain size was increased with increasing Sn doping. Therefore, it can be concluded that there is a good agreement between SEM and XRD pattern.

3.2. Degradation of PHE using synthesized nanopowders

Fig. 3 shows comparison of the activities of ZnO and 10% SnO_2 doped ZnO nanopowders. The experimental results showed that the 10% SnO_2 doped ZnO had high

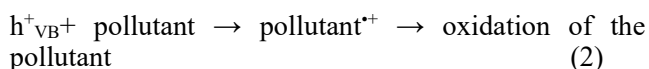
photocatalytic activity and its photocatalytic efficiency was higher than pure ZnO. Thus, subsequent experiments were carried out with 10% SnO_2 doped ZnO.

3.3. Effect of irradiation time

The required duration for the complete photocatalytic degradation of PHE was studied based on the duration of the catalyst irradiation to the UV source. Catalyst irradiation time was from 30 min to 120 min. The results indicated that the highest degradation efficiency was obtained when the irradiation of photocatalyst continued up to 120 min for PHE under UV light source. The photodegradation efficiency increased with respect to irradiation time of photocatalyst and the results obtained are shown in Fig. 4.

3.4. Photocatalytic activity

Photo-catalyzed degradation of a pollutant in solution is initiated by the photoexcitation of the semiconductor, followed by the formation of electron-hole pair on the surface of (ZnO/SnO_2) catalyst (Eq. (1)). The high oxidative potential of the hole (h^+_{VB}) in the catalyst permits direct oxidation of the pollutant to reactive intermediates (Eq. (2)):



Another reactive intermediate, which is responsible for the degradation, is hydroxyl radical (OH^\bullet). It is either formed by decomposition of water (Eq. (3)) or by reaction of the hole with OH^- (Eq. (4)).

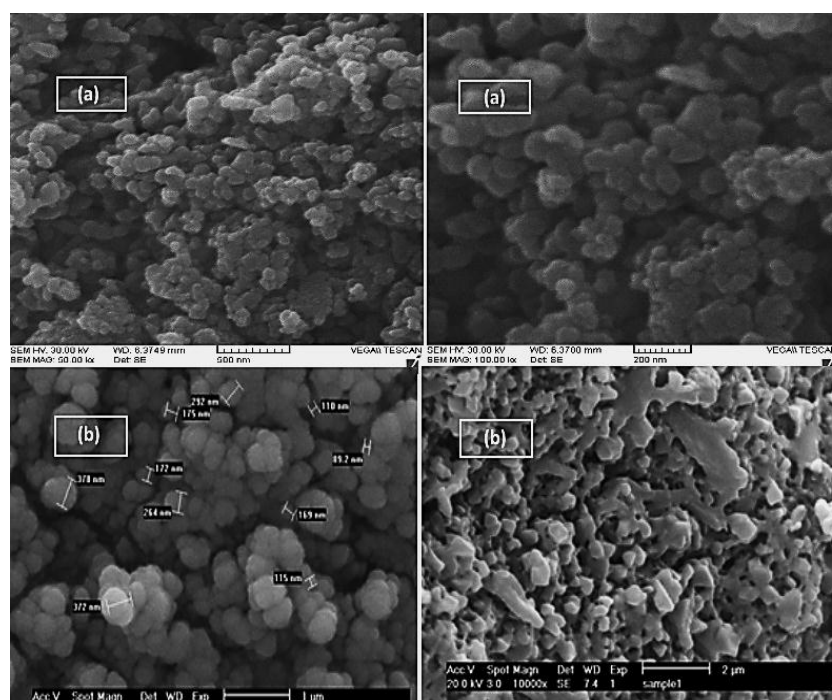


Fig. 2. SEM image of: (a) ZnO, (b) 10% SnO_2/ZnO .

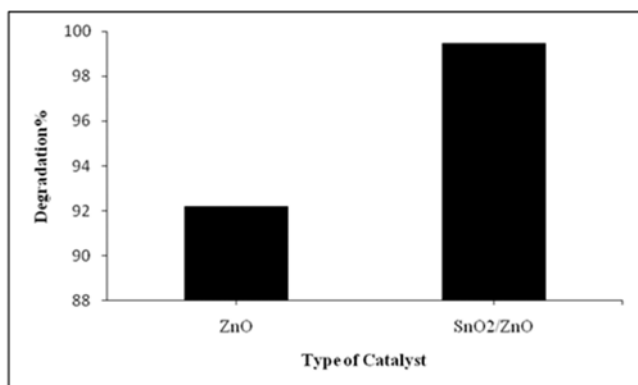


Fig. 3. comparison of the activities of ZnO and SnO₂/ZnO.

Conditions: PHE=20mg/L, ZnO and SnO₂/ZnO= 0.28 g/L, K₂S₂O₈=3 mM, pH=7.0, irradiation time=90 min, V_t=25 mL.

It should be emphasized that hydroxyl radical is an extremely strong, non-selective oxidant ($E_0 = +3.06$ V), which leads to the partial or complete mineralization of several organic chemicals [34]:



3.5. Effect of catalyst concentration

In order to determine the effect of catalyst loading, the experiments were performed by varying catalyst concentration from 0.04 to 0.52 g/L solutions of 20 mg/L at natural pH and 3m M K₂S₂O₈. The degradation efficiency for catalysts loading for PHE is depicted in Fig. 5. This Figure reveals that initial slopes of the curves increase greatly by increasing catalyst loading from 0.04 to 0.12 g/L for PHE. The rate of degradation remains then almost constant. In case of PHE maximum degradation, it was observed that with 0.28 g/L, and thereafter, increase in the dose of catalyst had no effect.

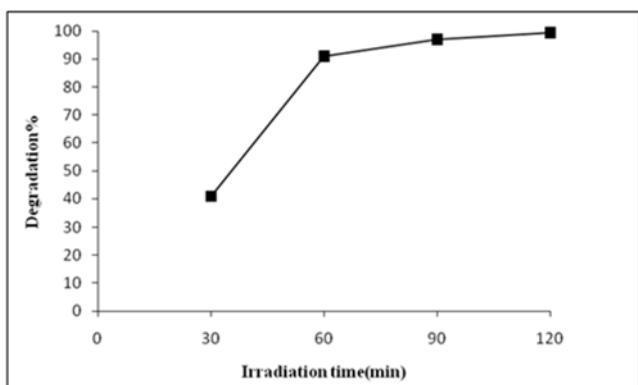


Fig. 4. Effect of irradiation time on the photodegradation efficiency.

Conditions: PHE =20 mg/L, SnO₂/ZnO= 0.28 g/L, K₂S₂O₈=3 mM, pH=7.0, V_t=25 mL.

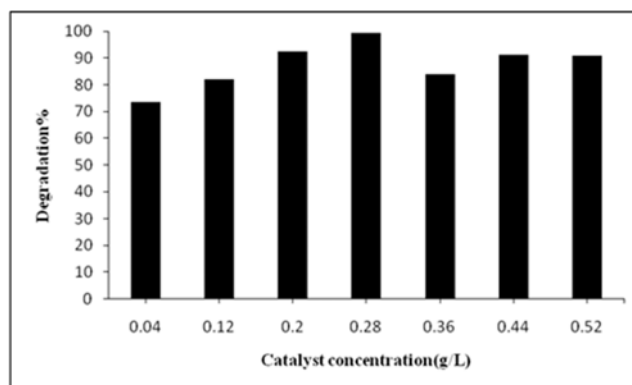


Fig. 5. Effect of catalyst concentration on the photodegradation efficiency.

Conditions: PHE =20 mg/L, K₂S₂O₈=3 mM, pH=7.0, irradiation time=120 min, V_t=25 mL.

The photocatalytic destruction of other organic pollutants has also been reported to exhibit a similar dependency on the catalyst dose [38]. This can be explained by considering that the optimum catalyst loading is dependent on the initial solute concentration. It has been reported that an increase in the catalyst dosage leads to an increase in the total active surface area, hence availability of more active sites on the catalyst surface [39]. At the same time, due to an increase in turbidity of the suspension with a high dose of photocatalyst, there will be a decrease in the penetration of UV light, and hence, the photoactivated volume of suspension decreases [40]. Thus, it can be concluded that a higher dose of catalyst may not be useful both in view of aggregation and as reduced irradiation field due to light scattering. Therefore, the catalyst doses of 0.28 and 0.12 g/L were fixed for PHE respectively in the course of further studies.

3.6. Effect of pH

Fig. 6 shows the degradation efficiency of PHE as a function of pH. The maximum degradation efficiency was obtained in pH 7.0.

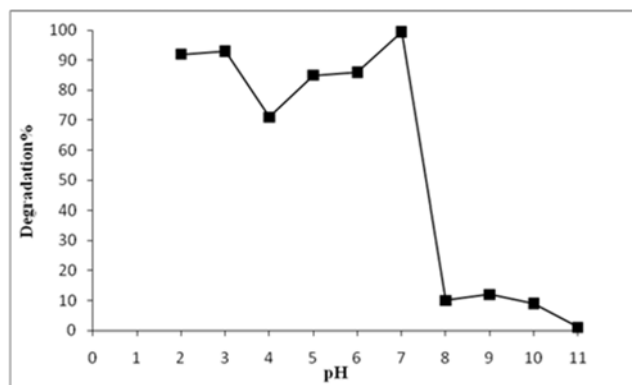


Fig. 6. Effect of pH on the photodegradation efficiency.

Conditions: PHE =20 mg/L, SnO₂/ZnO= 0.28 g/L, K₂S₂O₈=3 mM, irradiation, time=120 min, V_t=25 mL.

Wastewater containing pharmaceuticals is discharged at different pH; therefore, it is important to study the role of pH on degradation of PHE. To study the effect of pH on the degradation efficiency, experiments were carried out at various pH values, ranging from 2.0 to 11.0 for constant drug concentration (20 mg/L) and catalyst loading (0.28 and 0.12 g/L, respectively, for PHE). The interpretation of pH effects on the efficiency of the photocatalytic degradation process is a very difficult task because of its multiple roles [39]. In acidic and neutral solutions photodegradation efficiency was more than in alkaline solutions. The pK_a phenylephrine hydrochloride is 8.97. In the pH less than 9 the concentration of cationic form is more than molecular form and solubility of PEH increased, so the degradation by photocatalyst was done as well. But, in the basic media (pH more than 9), the concentration of cationic form is less than the molecular form and solubility PEH decreased, so the degradation of PEH by photocatalyst stopped. Meanwhile, it was found that the zinc oxide suspension could not be electrostatically stabilized in the preset pH range between 7.2 and 12 due to the transformation of colloidal $Zn(OH)_{2(s)}$ particles to $Zn(OH)_{2(aq)}$ [41]. This result was obtained according to experiment data, because we obtained the maximum degradation of PEH in pH 7.0.

3.7. Effect of concentration of PHE

After optimizing the pH conditions and the catalyst amount (pH=7.0 and catalyst amount 0.28 g/L for PHE), the photocatalytic degradation of PHE was carried out by varying the initial concentrations of the PHE from 10 to 60 mg/L. As the concentration of the drug increased, the rate of photodegradation decreased indicating either an increase in the catalyst dose or in the time span for the complete removal. Fig. 7 depicts the time dependent graph of degradation of PHE (10-60 mg/L). In the case of PHE, for drug solution of 20 mg/L, almost 99.4% degradation occurred within 120 min. The possible explanation for this behavior is that as the initial concentration of the drug increases, the

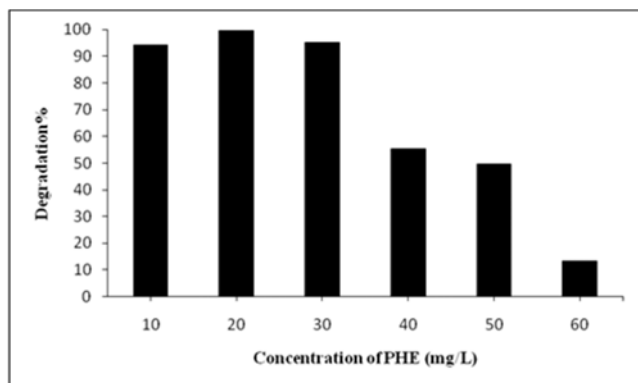


Fig. 7. Effect of concentration of PHE.

Conditions: $SnO_2/ZnO = 0.28$ g/L, $K_2S_2O_8 = 3$ mM, pH=7.0, irradiation time=120 min, $V_r = 25$ mL.

path length of the photons entering the solution decreases and in low concentration the reverse effect is observed, thereby, increasing the number of photon absorption by the catalyst in lower concentration [42].

3.8. Effect of Effect of $K_2S_2O_8$

In this study, the effect of persulfate ion on the photocatalytic degradation of the PHE was investigated (concentration of $K_2S_2O_8$: 1 to 7mM). The data are presented in Fig. 8. The percentage of PHE degradation increased with increasing the amount of persulfate ion concentration and achieved 99.4% within 120 min irradiation time at 3mM persulfate ion concentration. It is a beneficial oxidizing agent in photocatalytic detoxification because $SO_4^{\cdot-}$ is formed from the oxidant by reaction (eqs. (6) and (7)) with the semiconductor generated electrons (e^-_{CB}).



The sulfate radical anion ($SO_4^{\cdot-}$) is a strong oxidant ($E_0 = 2.6$ eV) and engages in the following three possible modes of reactions with organic compounds. (i) by abstracting a hydrogen atom from saturated carbon. (ii) by adding to unsaturated or aromatic carbon and (iii) by removing one electron from the carboxylate anion and from certain neutral molecules [43]. In addition, it can trap the photogenerated electrons and or generate hydroxyl radical [43–45]. Hydroxyl and sulfate radical anions (eqs (8) and (9)) are powerful oxidants that can degrade the pollutant molecules at higher rate. The $SO_4^{\cdot-}$ has the unique nature of attacking the pollutant molecule at various positions and hence the fragmentation of the pollutant molecules is rapid [13].

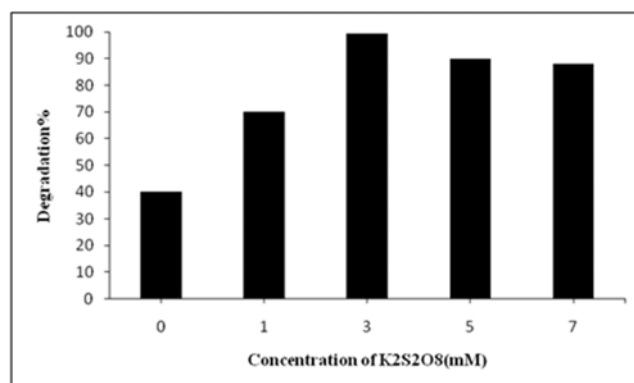
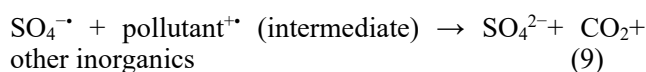
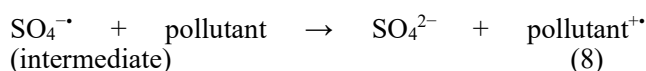


Fig. 8. Effect of $K_2S_2O_8$ on the photodegradation efficiency.

Conditions: PHE =20 mg/L, $SnO_2/ZnO = 0.28$ g/L, pH=7.0, irradiation time=120 min, $V_r = 25$ mL.

4. Conclusions

ZnO and 10 %SnO₂ doped ZnO powders were prepared by the sol-gel method. Comparison of photocatalytic activity of ZnO and 10 % SnO₂ doped ZnO clearly indicated that 10 %SnO₂ doped ZnO is the most active photocatalyst for degradation of PHE. Experimental results also indicated that degradation of drug was facilitated in the presence of the catalyst and favored the basic region. The initial rate of photodegradation increased with an increase in the catalyst dose up to an optimum loading. However, further increase in the catalyst dose showed no effect. As the initial concentration of PHE increased, the rate of degradation decreased in each pollutant. The optimal degradation conditions of 20 ppm PHE were: 0.28 g/L catalyst, pH 7.0, 3mM K₂S₂O₈ and irradiation time of 120 min. Under optimal degradation conditions, the photodegradation of PHE was obtained to be (99.4 ± 1.0) %.

Acknowledgment

The financial support provided by the Islamic Azad University of Lahijan is greatly acknowledged.

References

- [1] D. Calamari, E. Zuccato, S. Castiglioni, R. Bagnati, R. Fanelli, *Environ. Sci. Technol.* 37 (2003) 1241-1248.
- [2] C.G. Daughton, T.A. Ternes, *Environ. Health Perspect. Suppl.* 107 (1999) 907-938.
- [3] B. Halleing-Sorensen, S.N. Nielsen, P.F. Lanzky, F. Ingerslev, H.C.H. Lutzhoft, S.E. Jorgensen, *Chemosphere* 36 (1997) 357-394.
- [4] O.A.H. Jones, N. Volvlvoulis, J.N. Lester, *Environ. Technol.* 22 (2001) 1383-1394.
- [5] T.A. Ternes, *Wat. Res.* 32 (1998) 3245-3260.
- [6] M. Abu Tariq, M. Faisal, M. Muneer, D.W. Bahnemann, *J. Mol. Catal. A: Chem.* 265 (2007) 231-236.
- [7] D.W. Bahnemann, M. Muneer, M.M. Haque, *Catal. Today* 124 (2007) 133-148.
- [8] M.M. Haque, M. Muneer, D.W. Bahnemann, *Environ. Sci. Technol.* 40 (2006) 4766-4770.
- [9] J. Blanco-Galvez, P. Fernandez-Ibanez, S. Malato-Rodriguez, *J. Sol. Energy Eng.* 129 (2007) 4-15.
- [10] M.H. Habibi, E. Askari, *Iran. J. Catal.* 1 (2011) 41-44.
- [11] H. Faghihian, A. Bahranifard, *Iran. J. Catal.* 1 (2011) 45-50.
- [12] M.A. Behnajady, N. Modirshahla, R. Hamzayi, *J. Hazard. Mater.* 133 (2006) 226-232.
- [13] B. Neppolian, H.C. Choi, S. Sakthivel, B. Arabindoo, V. Murugesan, *J. Hazard. Mater.* 89 (2002) 303-317.
- [14] I.K. Konstantinou, T.A. Albanis, *Appl. Catal. B* 42 (2003) 319-335.
- [15] S. Senthilkumar, K. Porkodi, R. Vidyalakshmi, *J. Photochem. Photobiol.* 170 (2005) 225-232.
- [16] S. Sakthivel, B. Neppolian, B.V. Shankar, B. Arabindoo, M. Palanichamy, V. Murugesan, *Sol. Energy Mater. Sol. Cells* 77 (2003) 65-82.
- [17] C. Wang, X.M. Wang, B.Q. Xu, J.C. Zhao, B.X. Mai, P.A. Peng, G.Y. Sheng, J.M. Fu, *J. Photochem. Photobiol. A* 168 (2004) 47-52.
- [18] S. Sakthivel, S.U. Geissen, D.W. Bahnemann, V. Murugesan, A. Vogelpohl, *J. Photochem. Photobiol. A* 148 (2002) 283-293.
- [19] I. Eswaramoorthi, V. Sundaramurthy, A.K. Dalai, *Appl. Catal. A* 313 (2006) 22-34.
- [20] H.C. Yang, F.W. Chang, L.S. Roselin, *J. Mol. Catal. A: Chem.* 276 (2007) 184-196.
- [21] D.H. Yoon, J.H. Yu, G.M. Choi, *Sens. Actuators B* 46 (1998) 15-23.
- [22] H. R. Pouretedal, M. Ahmadi, *Iran. J. Catal.* 3 (2013) 149-155.
- [23] B. Khodadadi, M. Bordbar, *Iran. J. Catal.* 6 (2016) 37-42.
- [24] F. Xu, P. Zhang, A. Navrotsky, Z.Y. Yuan, T.Z. Ren, M. Halasa, B.L. Su, *Chem. Mater.* 19 (2007) 5680-5686.
- [25] M.R. Hoffmann, S.T. Martin, W.Y. Choi, D.W. Bahnemann, *Chem. Rev.* 95 (1995) 69-96.
- [26] I. Bedjat, P.V. Kamat, *J. Phys. Chem.* 99 (1995) 9182-9188.
- [27] M.K. Nowotny, L.R. Sheppard, T. Bak, J. Nowotny, *J. Phys. Chem. C* 112 (2008) 5275-5300.
- [28] S. Anandan, A. Vinu, T. Mori, N. Gokulakrishnan, P. Srinivasu, V. Murugesan, K. Ariga, *Catal. Commun.* 8 (2007) 1377-1382.
- [29] J.K. Zhou, L. Lv, J. Yu, H.L. Li, P.Z. Guo, H. Sun, X.S. Zhao, *J. Phys. Chem. C* 112 (2008) 5316-5321.
- [30] Y. Zheng, L. Zheng, Y. Zhan, X. Lin, Q. Zheng, K. Wei, *Inorg. Chem.* 46 (2007) 6980-6986.
- [31] E. A. Davis, N. F. Mott, *Phil. Mag.* 22 (1970) 903-922.
- [32] F. Jahan, M.H. Islam, B.E. Smith, *Sol. Energy Mater. Sol. Cells* 37 (1995) 283-293.
- [33] (a) A. Hagfeldt, M. Gratzel, *Chem. Rev.* 95 (1995) 49-68. (b) C.F. Lin, C.H. Wu, Z.N. Onn, *J. Hazard. Mater.* 154 (2008) 1033-1039. (c) R. Memming, *Electrochim. Acta* 25 (1980) 77-88. (d) R. Vogel, P. Hoyer, H. Weller, *J. Phys. Chem.* 98 (1994) 3183-3188.
- [34] Y. Hu, X.H. Zhou, Q. Han, Q.X. Cao, Y.X. Huang, *Mater. Sci. Eng. B* 99 (2003) 41-43.
- [35] M. Giahi, H. Taghavi, S. Saadat, A. Abdolazadeh Ziabari, *Optoelectron. Adv. Mater. Rapid Commun.* 9 (2015) 1114-1119.
- [36] M. Giahi, S. Saadat Niavol, H. Taghavi, M. Meskinfam, *Russ. J. Phys. Chem. A* 89 (2015) 2432-2437.
- [37] M. Giahi, N. Badalpoor, S. Habibi, H. Taghavi, *Bull. Korean Chem. Soc.* 34 (2013) 2176-82.
- [38] N. Daneshvar, D. Salari, A.R. Khataee, *J. Photochem. Photobiol. A* 157 (2003) 111-116.
- [39] M.S.T. Goncalves, A.M.F. Oliveira-Campos, E.M.M.S. Pinto, P.M.S. Plasencia, M.J.R.P. Queiroz, *Chemosphere* 39 (1999) 781-786.
- [40] A. Akyol, H.C. Yatmaz, M. Bayramoglu, *Appl. Catal. B* 54 (2004) 19-24.
- [41] A. Degen, M. Kosec, *J. Eur. Ceram. Soc.* 20 (2000) 667-673.
- [42] R.J. Davis, J.L. Gainer, G.O. Neal, I.W. Wu, *Water Environ. Res.* 66 (1994) 50-53.

- [43] C. Nasr, K. Vinodgopal, S. Kotchandani, A.K. Chattopadhyay, P.K. Kamat, *Chem. Intermed.* 23 (1997) 219-231.
- [44] E. Pelizzetti, V. Carlin, C. Minero, M. Gratzel, *New J. Chem.* 15 (1991) 351-359.
- [45] C. Minero, E. Pelizzetti, S. Malato, J. Blanco, *Chemosphere* 26 (1993) 2103-2119.